Relaxation dynamics near nonequilibrium stationary states in Brownian ratchets

Hyung-June Woo
Department of Chemistry, University of Nevada, Reno, Nevada 89557, USA
(Received 27 September 2008; revised manuscript received 23 November 2008; published 2 February 2009)

A comprehensive study of the static and dynamical properties of a representative stochastic model of Brownian ratchet effects for molecular motors is reported. The model describes Brownian motions on two periodic potentials under static and time-dependent forces, where there are two distinct locations of chemical reactions coupling the levels with reversible rates within a period. Complete stationary properties have been obtained analytically for arbitrary potentials under external force. Dynamical relaxation properties near nonequilibrium stationary states were examined by considering the response function of velocity upon time-dependent external force, expressed in terms of the conditional probability density of the model. The latter is fully calculated using a systematic numerical method using matrix diagonalization, which is easily generalized to more complicated models for studying both static and dynamical properties. The behavior of the time-dependent response examined for model potentials suggests that the characteristic relaxation time near stationary states generally decreases linearly with respect to increasing velocity as one goes away from equilibrium via an increase in chemical potential of fuel species, a prediction testable in single molecule experiments.

DOI: 10.1103/PhysRevE.79.021101 PACS number(s): 05.40.−a, 05.10.Gg, 87.16.Nn

I. INTRODUCTION

Driven systems in nanoscale exhibit many nontrivial features distinct from properties in equilibrium. Of particular interest are those seen in systems exhibiting chemomechanical coupling including molecular motor proteins [1], where chemical free energy of fuel species such as adenosine triphosphate (ATP) is converted into mechanical work. Modern single molecule experiments [2–4] now provide data that can be used to aid and test theoretical treatments. Basic theoretical framework for such treatments is provided by the stochastic dynamical models, including continuous variable Fokker-Planck formalisms [5–22]. To varying degrees the models incorporate the concept of Brownian ratchet effects, where thermal fluctuations are harnessed via external controls such as chemical or biochemical reactions driven by nonequilibrium conditions.

Most of the studies using stochastic models of motors, however, have so far mainly been focused on static properties, and relatively little is known about the dynamical relaxation behavior exhibited by such systems away from equilibrium. Basic stochastic differential equations have unique stationary solutions [23,24] to which all transient states evolve in the long time limit. Characteristics of this relaxation behavior, intimately connected to spontaneous fluctuations only when the stationary state is an equilibrium state, potentially have many important implications to the behavior of nanoscale motors and devices: Single molecule experiments using optical tweezers often probe responses in velocity to changes in external force, while control of artificial nanoscale devices would critically depend on their response characteristics to external perturbations.

In this paper, we systematically examine the dynamical relaxation behavior of nanoscale motors toward nonequilibrium stationary states using a representative version of Brownian ratchets [11,12], containing two level periodic potentials coupled by reactions. Stationary properties of this model have previously been studied numerically for a choice of piecewise linear potentials in Ref. [25]. The model and its basic stochastic dynamics are defined in the next section, and in Sec. III, the analytical solution for stationary properties valid for arbitrary potentials and external force is derived. In Sec. IV, linear response theory is first applied to relate the response function of velocity near nonequilibrium stationary states to the probability densities of the model. A general procedure for calculating both the time-dependent conditional probability and stationary properties is then developed. Features of the response function and its characteristic relaxation time are examined as functions of model parameters governing the departure from equilibrium in Sec. V. Section VI contains concluding discussions.

II. TWO LEVEL MODEL

The model adopted is illustrated in Fig. 1, which is a version of fluctuating potential ratchet models [9,11]: A one-dimensional stochastic variable x undergoes Brownian motion under two potentials

$$G_n(x) = G_n^{(0)}(x) - f_0 x \tag{1}$$

with $n=1,2$ and a static external force f_0. The potentials $G_n^{(0)}$ are periodic with the period taken as the unit of length, such that $G_n^{(0)}(x+l)=G_n^{(0)}(x)$ with integer l. The two levels are coupled by reactions localized at two positions x_1 and x_2 within a period, with rates k_1 (k_{-1}) for the transition $n=2 \rightarrow 1$ $(1 \rightarrow 2)$ at x_1, and k_2 (k_{-2}) for the transition $n=1 \rightarrow 2$ $(2 \rightarrow 1)$ at x_2. For processive motors where x is the displacement of a motor complex (or the rotation angle for rotary motors), the two levels G_1 and G_2 may correspond to bound and unbound states or different conformational states of the protein.

The average value of an observable of interest $A_n(x,t)$ is given by

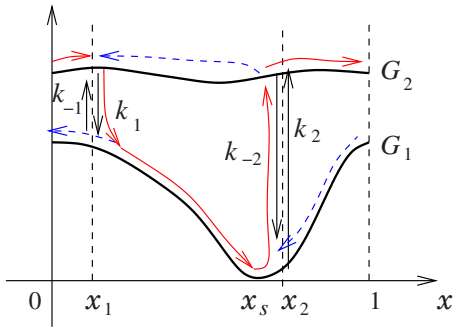

FIG. 1. (Color online) Two level model of a spatial coordinate $0 \leqslant x \leqslant 1$ in periodic boundaries with two potentials G_1 and G_2, coupled at $x=x_1$ and $x=x_2$ each with rates $k_{\pm 1}$ and $k_{\pm 2}$. Location of the minimum of model potential depicted is denoted as x_s [Eqs. (62) and (63)]. Curved arrows illustrate an example of local fluxes resulting from a k_2 value larger than that for equilibrium condition; solid (red) arrows indicate fluxes larger in magnitude than those with dashed (blue) arrows, and the velocity is positive, while the reactive flux is in counterclockwise direction.

$$\langle A \rangle = \sum_n \int dx A_n(x,t) P_n(x,t), \tag{2}$$

where the sum is over states $n=1,2$, the integration is over all accessible ranges of x, and $P_n(x,t)$ is the probability density to find the system on the level n and position x at time t. Considerations of the time evolution of $P_n(x,t)$ are facilitated via the conditional probability $P_{nm}(x,t|x_0,0)$ to observe x on the level n at time t given that the system was at x_0 at $t=0$ on the level m. This conditional probability is the Green's function for $P_n(x,t)$ satisfying

$$P_n(x,t) = \sum_m \int dx_0 P_{nm}(x,t|x_0,0) P_m(x_0,0) \tag{3}$$

with the initial condition

$$P_{nm}(x,0|x_0,0) = \delta_{nm}\delta(x-x_0). \tag{4}$$

The time evolution of P_{nm} is governed by

$$\partial_t \mathsf{P}(x,t|x_0,0) = \hat{\mathsf{L}}(x,t) \cdot \mathsf{P}(x,t|x_0,0), \tag{5}$$

where we have introduced a matrix notation with

$$\mathsf{P} = \begin{bmatrix} P_{11} & P_{12} \\ P_{21} & P_{22} \end{bmatrix} \tag{6}$$

and $\hat{\mathsf{L}}$ is a matrix of Fokker-Planck operators that we write as

$$\hat{\mathsf{L}}(x,t) = \hat{\mathsf{L}}_0(x) + \hat{\mathsf{L}}'(x,t), \tag{7}$$

where $\hat{\mathsf{L}}'$ represents contributions due to time-dependent external perturbations. The time-independent part of the operator can be written as (Fig. 1)

$$\hat{\mathsf{L}}_0 = -\hat{\Omega} + \delta(x-x_1)\mathsf{K}_1 + \delta(x-x_2)\mathsf{K}_2, \tag{8}$$

where

$$\hat{\Omega} = \partial_x \begin{bmatrix} -G_1' - \partial_x & 0 \\ 0 & -G_2' - \partial_x \end{bmatrix} \equiv \partial_x \hat{\mathsf{J}} \tag{9}$$

and $G_n' \equiv dG_n/dx$. The two terms in the diagonal elements of Eq. (9) represent fluxes due to active transport in the overdamped regime and diffusion, respectively, and we have chosen the inverse diffusion coefficient and k_BT as the units of time and energy to simplify the notation. The two singular terms in Eq. (8) with

$$\mathsf{K}_1 = \begin{bmatrix} -k_{-1} & k_1 \\ k_{-1} & -k_1 \end{bmatrix}, \quad \mathsf{K}_2 = \begin{bmatrix} -k_2 & k_{-2} \\ k_2 & -k_{-2} \end{bmatrix} \tag{10}$$

represent the contributions to the flux due to reactions. Since a time-dependent perturbation $f(t)$ to the static force f_0 would add to $-G_n'$ in Eq. (9), the operator representing the perturbation can be written as

$$\hat{\mathsf{L}}'(x,t) = -f(t)\mathsf{I}\partial_x, \tag{11}$$

where I is the identity matrix.

III. STATIONARY PROPERTIES

Irrespective of the initial condition at $t=0$, the probability density approaches the unique stationary distribution in the long time limit when $f(t)=0$,

$$\mathsf{P}(x,\infty|x_0,0) = [\bar{\mathbf{P}}(x)\ \bar{\mathbf{P}}(x)] \equiv \begin{bmatrix} \bar{P}_1(x) & \bar{P}_1(x) \\ \bar{P}_2(x) & \bar{P}_2(x) \end{bmatrix}. \tag{12}$$

The stationary density $\bar{\mathbf{P}}(x)$ satisfies

$$\hat{\mathsf{L}}_0 \cdot \bar{\mathbf{P}} = 0. \tag{13}$$

From Eq. (8), $\hat{\mathsf{L}}_0 = -\partial_x \hat{\mathsf{J}}$ for $x \neq x_n$. For decoupled levels ($k_{\pm n}=0$), it can be shown that the stationary solution is periodic even when $f_0 \neq 0$ (Ref. [23], p. 288). We assume $\bar{P}_n(x+1) = \bar{P}_n(x)$ to be valid generally, which is validated by the solution obtained and its uniqueness. It is therefore sufficient to limit the range of x to $0 \leqslant x \leqslant 1$ with $\Sigma_l \bar{P}(x+l) \to \bar{P}(x)$. Dividing the period of x into three nonsingular regions $0 \leqslant x \leqslant x_1$ ($j=1$), $x_1 \leqslant x \leqslant x_2$ ($j=2$), and $x_2 \leqslant x \leqslant 1$ ($j=3$), Eqs. (9) and (13) give

$$\left(-G_n' - \frac{d}{dx}\right)\bar{P}_n^{(j)} = J_n^{(j)} = \text{const}, \tag{14}$$

where $J_n^{(j)}$ is the stationary flux on level n within the region j. Imposing boundary conditions at $x=0, x_1, x_2, 1$ to the general functional form of the solution to (14) [21,22], the following solution can be obtained (Appendix A):

$$\bar{P}_1 = Ae^{-G_1(x)}\begin{cases} 1+\dfrac{(1-e^{-f_0})w_1}{g_1+h_1}-\dfrac{w_1m_1'm_2}{m_1g_1Q}\Gamma_1-\left(\dfrac{1-e^{-f_0}}{g_1+h_1}-\dfrac{m_1'm_2}{m_1g_1Q}\Gamma_1\right)\displaystyle\int_0^x dx'e^{G_1(x')} & (0\leqslant x\leqslant x_1),\\ 1-\left(\dfrac{1-e^{-f_0}}{g_1+h_1}+\dfrac{m_1'm_2}{m_1h_1Q}\Gamma_1\right)\displaystyle\int_{x_1}^x dx'e^{G_1(x')} & (x_1\leqslant x\leqslant x_2),\\ \dfrac{m_1'}{m_1}\left(1-\dfrac{m_2}{Q}\Gamma_1\right)-\left(\dfrac{1-e^{-f_0}}{g_1+h_1}-\dfrac{m_1'm_2}{m_1g_1Q}\Gamma_1\right)\displaystyle\int_{x_2}^x dx'e^{G_1(x')} & (x_2\leqslant x\leqslant 1), \end{cases}$$

$$\bar{P}_2 = \frac{A}{Q}e^{-G_2(x)}\begin{cases} e^{f_0}M+\dfrac{(1-e^{f_0})u_2}{g_2h_2}F-\dfrac{e^{f_0}u_2m_1'}{g_2}\Gamma_3-\left(\dfrac{1-e^{-f_0}}{g_2h_2}F+\dfrac{m_1'}{g_2}\Gamma_3\right)\displaystyle\int_0^x dx'e^{G_2(x')} & (0\leqslant x\leqslant x_1),\\ L-\left(\dfrac{1-e^{-f_0}}{g_2h_2}F-\dfrac{m_1'}{h_2}\Gamma_2\right)\displaystyle\int_{x_1}^x dx'e^{G_2(x')} & (x_1\leqslant x\leqslant x_2),\\ M-\left(\dfrac{1-e^{-f_0}}{g_2h_2}F+\dfrac{m_1'}{g_2}\Gamma_3\right)\displaystyle\int_{x_2}^x dx'e^{G_2(x')} & (x_2\leqslant x\leqslant 1), \end{cases} \tag{15}$$

where

$$\Gamma_1 = c_1k_2d_2k_1-\frac{m_1m_2'}{m_1'm_2}c_2k_{-2}d_1k_{-1}, \tag{16a}$$

$$\Gamma_2 = c_1k_2d_2k_1-\frac{m_1}{m_1'}c_2k_{-2}d_1k_{-1}, \tag{16b}$$

$$\Gamma_3 = c_1k_2d_2k_1-\frac{m_1e^{-f_0}}{m_1'}c_2k_{-2}d_1k_{-1}, \tag{16c}$$

$$M = m_1'm_2'c_1k_2+m_1m_2'd_1k_{-1}+c_1k_2(m_1'd_2k_1+m_2'd_1k_{-1}), \tag{17a}$$

$$L = m_1'm_2c_1k_2+m_1m_2d_1k_{-1}+d_1k_{-1}(m_1c_2k_{-2}+m_2c_1k_2), \tag{17b}$$

$$Q = m_1m_2'c_2k_{-2}+m_1m_2d_2k_1+d_2k_1(m_1c_2k_{-2}+m_2c_1k_2), \tag{17c}$$

$$F = c_1k_2(d_1k_{-1}+m_1')+m_1d_1k_{-1}, \tag{17d}$$

$d_n=e^{-G_n(x_1)}$, $c_n=e^{-G_n(x_2)}$, $w_n=\int_0^{x_1}dxe^{G_n(x)}$, $h_n=\int_{x_1}^{x_2}dxe^{G_n(x)}$, $u_n=\int_{x_2}^{1}dxe^{G_n(x)}$, $g_n=u_n+e^{-f_0}w_n$, $m_n=1/h_n+1/g_n$, and $m_n'=1/h_n+e^{-f_0}/g_n$. The normalization constant A is determined by $\int_0^1dx(\bar{P}_1+\bar{P}_2)=1$. The stationary velocity $v_0=J_1^{(j)}+J_2^{(j)}$ is independent of j,

$$\frac{v_0}{A} = (1-e^{-f_0})\left(\frac{1}{g_1+h_1}+\frac{F}{g_2h_2Q}\right)+\frac{m_1'}{m_1Q}\left(\frac{m_2}{h_1}\Gamma_1-\frac{m_1}{h_2}\Gamma_2\right). \tag{18}$$

Also of interest is the reactive flux r_0, or the "ATPase rate," the rate of ATP consumption when k_2 corresponds to the ATP binding and/or hydrolysis step. It is defined as the flux of $2\leftarrow 1$ transition at the reaction location x_2,

$$r_0 = Am_1'm_2\frac{\Gamma_1}{Q}. \tag{19}$$

The corresponding flux at x_1 is $-r_0$, such that the total net flux between the two levels vanishes in the stationary state. We also note that v_0 and r_0 are linearly related with respect to changes in $k_{\pm n}$,

$$v_0 = A(1-e^{-f_0})\left(\frac{1}{g_1+h_1}+\frac{F}{g_2h_2Q}\right)-A\frac{m_1'\Gamma_2}{h_2Q}+\frac{r_0}{m_1h_1}. \tag{20}$$

This linear dependence between the velocity and ATPase rate has previously been noted via regression of the numerical solution using sawtooth potentials in Ref. [25].

We can identify the two terms of Eq. (18) for velocity as the main contributions due to force and reactions, respectively. If f_0 is increased with constant rates, v_0 increases mainly in response to the mechanical driving force, while the reactive flux r_0 remains nearly constant. On the other hand, if one for instance increases k_2 away from its equilibrium value while keeping other rates and f_0 constant, both v_0 and r_0 increase.

A. Decoupled level

A special case of interest is when rate constants vanish and the two levels are decoupled. The model then reduces to the description of Brownian motion on a periodic potential under external force, which has been analyzed in detail by Risken [23]. Setting $k_2=0$ and $k_{-1}=0$ such that the level $n=2$ is inaccessible from $n=1$, Eq. (15) becomes

$$\bar{P}_1(x) = Ae^{-G_1(x)}\left(1 - \frac{1-e^{-f_0}}{g_1+h_1}\int_{x_1}^{x} dx' e^{G_1(x')}\right)$$
$$= Ae^{-G_1(x)}\left(1 - \frac{1-e^{-f_0}}{\int_0^1 dx' e^{G_1(x')}}\int_0^{x} dx' e^{G_1(x')}\right)$$
$$= A' e^{-G_1(x)}\int_x^{x+1} dx' e^{G_1(x')}, \tag{21}$$

where in the second line we have set $x_1=0$ since x_n are arbitrary without reactions, and $G_1(x+1)=G_1(x)-f_0$ was used in the third line with $A'=A/\int_0^1 dx e^{G_1(x)}$. The third line is equivalent to Eq. (2.36) of Ref. [6]. The velocity can be obtained from Eq. (18), or read off as the negative of the coefficient of the second term in the second line of Eq. (21),

$$v_0 = \frac{A(1-e^{-f_0})}{\int_0^1 dx' e^{G_1(x')}}. \tag{22}$$

B. Zero force

As Eq. (21) makes it clear, equilibria on periodic potentials are in general precluded either with or without reactions if $f_0 \neq 0$. If $f_0=0$, Eq. (15) shows that the deviation of $\bar{P}_n$ from the equilibrium Boltzmann distribution is controlled by

$$\Gamma = c_1 k_2 d_2 k_1 - c_2 k_{-2} d_1 k_{-1} \tag{23}$$

with $\Gamma_1=\Gamma_2=\Gamma_3=\Gamma$. The detailed balance conditions at the two reaction locations x_1 and x_2 read $c_1k_2=c_2k_{-2}$ and $d_2k_1=d_1k_{-1}$, respectively (Fig. 1), which implies $\Gamma=0$, $M=L=Q$, and $\bar{P}_n(x)=Ae^{-G_n(x)}$. The stationary velocity at zero force simplifies to

$$v_0 = A\left(\frac{1}{h_1 g_2} - \frac{1}{h_2 g_1}\right)\frac{\Gamma}{Q}, \tag{24}$$

which is nonzero only if $\Gamma \neq 0$. Symmetry of the potentials and x_n values also can lead to $v_0=0$ irrespective of Γ: For example, if $x_1=0$, $x_2=1/2$, and $G_n(x)=G_n(1-x)$, $g_n=h_n$ and $v_0=0$.

For concreteness, we choose the rate k_2 to be the main step which drives the system out of equilibrium, and write

$$k_2 = k_2^{(0)} e^{\Delta\mu} \equiv (1+z)k_2^{(0)}, \tag{25}$$

where $k_2^{(0)}$ is the value of the rate satisfying detailed balance for $f_0=0$, and $\Delta\mu=\ln(1+z)$ is the difference in chemical potential of the fuel species from its equilibrium value. If certain values of k_1 and $k_2^{(0)}$ are chosen and the reverse rates are given by

$$k_{-2} = e^{-[G_1^{(0)}(x_2)-G_2^{(0)}(x_2)]}k_2^{(0)}, \tag{26a}$$

$$k_{-1} = e^{-[G_2^{(0)}(x_1)-G_1^{(0)}(x_1)]}k_1, \tag{26b}$$

the single parameter z ($[\mathrm{ATP}]-[\mathrm{ATP}]_{\mathrm{eq}}$ in the buffer) can describe the departure from equilibrium ($z=0$). From Eqs. (16) and (17c), it is clear that Eqs. (24) and (19) lead to a Michaelis-Menten-type kinetics with respect to z. Equation (24), in particular, is expected to be useful in optimizing the maximum velocity with respect to potentials and reaction locations in designing artificial motors.

IV. DYNAMICAL RELAXATION

A. Linear response theory

With a small but nonvanishing perturbation $f(t)$, the velocity $v(t)$ would show small deviations from the stationary value given by Eq. (18). With Eq. (2), this velocity is given by [6]

$$v(t) = \sum_n \int dx[f(t) - G_n'(x)]P_n(x,t)$$
$$= f(t) - \sum_n \int dx G_n'(x) P_n(x,t), \tag{27}$$

where the normalization condition

$$\sum_n \int dx P_n(x,t) = 1 \tag{28}$$

was used. The temporal response $\Delta v = v(t) - v_0$, on the other hand, can be written as

$$\Delta v(t) = \int_{-\infty}^{t} dt' R(t-t') f(t'), \tag{29}$$

where $R(t)$ is the response function, a characteristic property of the stationary state on which $f(t)$ acts. The response function is independent of $f(t)$ in the linear response regime. We follow Ref. [23] to relate $R(t)$ to P below. Writing the probability density $P_n(x,t)$ as

$$\mathbf{P}(x,t) = \bar{\mathbf{P}}(x) + \mathbf{p}(x,t), \tag{30}$$

where $\mathbf{p}(x,t)$ is the time-dependent part due to perturbation, we have from Eq. (27),

$$\Delta v(t) = f(t) - \sum_n \int dx G_n'(x) p_n(x,t). \tag{31}$$

From Eqs. (5), (7), and (13), the time evolution of p_n is given by

$$\partial_t \mathbf{p}(x,t) = \hat{\mathsf{L}}(x,t)\cdot\mathbf{P}(x,t) \simeq \hat{\mathsf{L}}_0(x)\cdot\mathbf{p}(x,t) + \hat{\mathsf{L}}'(x,t)\cdot\bar{\mathbf{P}}(x), \tag{32}$$

where only the terms first order in perturbation have been kept. Equation (32) can be integrated as

$$\mathbf{p}(x,t) = \int_{-\infty}^{t} dt' e^{(t-t')\hat{\mathsf{L}}_0(x)}\cdot\hat{\mathsf{L}}'(x,t')\cdot\bar{\mathbf{P}}(x). \tag{33}$$

Equations (11), (29), (31), and (33) give

$$R(t) = \delta(t) + \int dx \mathbf{G}' \cdot e^{t\hat{\mathsf{L}}_0(x)} \cdot \partial_x \bar{\mathbf{P}}$$

$$= \delta(t) + \int\int dx dx_0 \mathbf{G}'(x) \cdot e^{t\hat{\mathsf{L}}_0(x)} \cdot \delta(x - x_0)\mathsf{I} \cdot \partial_{x_0} \bar{\mathbf{P}}(x_0)$$

$$= \delta(t) + \int\int dx dx_0 \mathbf{G}'(x) \cdot \mathsf{P}(x,t|x_0,0) \cdot \partial_{x_0} \bar{\mathbf{P}}(x_0), \quad (34)$$

where in the third line, the formal solution to Eqs. (5) and (4) was used.

From Eq. (14), we have $\partial_x \bar{P}_n^{(j)}(x) = -G_n'(x)\bar{P}_n^{(j)}(x) - J_n^{(j)}$, which allows us to write

$$R(t) = R_0(t) - \sum_{nm} \int\int dx dx_0 G_n'(x) P_{nm}(x,t|x_0,0) J_m(x_0), \quad (35)$$

where $J_m(x_0) = J_m^{(j)}$ for $x_0 \in j$, and

$$R_0(t) = \delta(t) - \sum_{nm} \int\int dx dx_0 G_n'(x) P_{nm}(x,t|x_0,0) \times G_m'(x_0)\bar{P}_m(x_0) \quad (36)$$

is the time correlation function of the force due to potentials. The second term in Eq. (35) is nonzero only away from equilibrium where $J_m \neq 0$ and represents the deviation from the standard fluctuation dissipation theorem. In Eq. (34), the δ function at $t=0$ represents the inertial response due to the external perturbation only: $v(t) = \eta^{-1} f(t)$ in the physical unit where η is the friction coefficient if $G_n(x) = 0$. The second term represents the effects of dissipative media to the response, which we expect is negative in sign, reducing the amount of instantaneous response one would have in the absence of dissipation.

Since we have reduced the range of x to one period only for the stationary solution in Sec. III, the integrals over x in this section are unrestricted, while those over x_0 are for $0 \leqslant x_0 \leqslant 1$. However, in the integrand of Eq. (34), $G_n'(x) = G_n^{(0)\prime}(x) - f_0$ is periodic in x, and by introducing the reduced conditional probability

$$\hat{P}_{nm}(x,t|x_0,0) = \sum_l P_{nm}(x+l,t|x_0,0), \quad (37)$$

the range of integration over x can be reduced to one period as well. This reduction also implies that although $\mathsf{P}(x,t|x_0,0)$ is not necessarily periodic with respect to x, $\hat{\mathsf{P}}(x,t|x_0,0)$ is always periodic. We will therefore drop the hat from $\hat{\mathsf{P}}$ in the following and restrict the spatial range of x to $0 \leqslant x \leqslant 1$.

B. Calculation of conditional probability

Equation (34) relates the response function to the probability densities of the model, and in particular, shows that its time dependence directly reflects that of P in the absence of perturbation. In this section, the full Fokker-Planck equation (5) is related to an eigenvalue equation, whose solution reflects the relaxation behavior of $\mathsf{P}(x,t|x_0,0)$ toward $\bar{\mathsf{P}}(x)$. Since the matrix of operators $\hat{\mathsf{L}}$ cannot easily be related to a Hermitian operator in the presence of reactions [Eq. (10)], the standard technique of transforming $\hat{\Omega}$ into a Schrödinger-type Hermitian operator [23], whose eigenfunctions form a complete set, is not readily applicable. We instead proceed by taking the Laplace transform of both sides of Eq. (5) with $\hat{\mathsf{L}}' = 0$ to get

$$s\tilde{\mathsf{P}}(x,s|x_0) - \hat{\mathsf{L}}_0(x) \cdot \tilde{\mathsf{P}}(x,s|x_0) = \delta(x - x_0)\mathsf{I}, \quad (38)$$

where

$$\tilde{\mathsf{P}}(x,s|x_0) = \int_0^\infty dt e^{-st} \mathsf{P}(x,t|x_0,0) \quad (39)$$

and Eq. (4) was used. We then use the Fourier series expansion for the x dependence,

$$\tilde{\mathsf{P}}(x,s|x_0) \simeq \sum_{l=-N}^{N} e^{2\pi i l x} \mathsf{C}_l, \quad (40)$$

where $\mathsf{C}_l = \mathsf{C}_l(s,x_0)$ are 2×2 matrices of complex coefficients. Substituting Eq. (40) into Eq. (38), multiplying on the left-hand side by $e^{-2\pi i k x}$ and integrating, we get

$$\sum_{l=-N}^{N} (s\delta_{kl}\mathsf{I} - \mathsf{L}_{kl}) \cdot \mathsf{C}_l = e^{-2\pi i k x_0}\mathsf{I}, \quad (41)$$

where $-N \leqslant k \leqslant N$,

$$\mathsf{L}_{kl} = \int_0^1 dx e^{-2\pi i k x} \hat{\mathsf{L}}_0 e^{2\pi i l x} = -\Omega_{kl} + e^{2\pi i (l-k)x_1}\mathsf{K}_1 + e^{2\pi i (l-k)x_2}\mathsf{K}_2 \quad (42)$$

and

$$\Omega_{kl} = \int_0^1 dx e^{-2\pi i k x} \hat{\Omega} e^{2\pi i l x} \quad (43)$$

is the matrix element of the operator $\hat{\Omega}$.

We introduce matrices of dimension $2(2N+1)$ formed by tensor products of Fourier coefficients $(k = -N, \ldots, N)$ and levels $(n = 1, 2)$, and rewrite Eq. (41) as

$$\mathbf{B}(s) \cdot \mathbf{C} = \mathbf{F}(x_0), \quad (44)$$

where

$$\mathbf{B}(s) = s\mathbf{I} - \mathbf{L}, \quad (45)$$

$\mathbf{L}$, $\mathbf{I}$, and $\mathbf{B}$ are $2(2N+1)$-dimensional square matrices, $\mathbf{C}$ and $\mathbf{F}$ are $2(2N+1)\times 2$ matrices, and their elements are

$$(\mathbf{L})_{\alpha,\beta} = (\mathsf{L}_{kl})_{nm}, \quad (46a)$$

$$(\mathbf{I})_{\alpha,\beta} = \delta_{\alpha,\beta}, \quad (46b)$$

$$(\mathbf{C})_{\alpha,m} = (\mathsf{C}_k)_{nm}, \quad (46c)$$

$$[\mathbf{F}(x_0)]_{\alpha,m} = e^{-2\pi i k x_0}\delta_{nm}, \quad (46d)$$

$$\alpha = 2(k+N)+n, \tag{46e}$$

$$\beta = 2(l+N)+m, \tag{46f}$$

where $-N \leqslant k, l \leqslant N$, $n,m=1,2$, and $1 \leqslant \alpha, \beta \leqslant 4N+2$. In the following, when roman and Greek indices appear together, Eqs. (46e) and (46f) are implicitly assumed. Equation (44) has the solution

$$\mathbf{C}(s) = \mathbf{B}^{-1}(s) \cdot \mathbf{F}(x_0). \tag{47}$$

To find $\mathbf{B}^{-1}$, we consider the eigenvalue equation for the matrix $\mathbf{L}$,

$$\mathbf{L} \cdot \mathbf{v}_\alpha = -\lambda_\alpha \mathbf{v}_\alpha. \tag{48}$$

Diagonalizability of the non-Hermitian matrix $\mathbf{L}$ is not guaranteed but could always be done numerically in our applications. From Eq. (45), we have

$$\mathbf{B} \cdot \mathbf{v}_\alpha = (s+\lambda_\alpha)\mathbf{v}_\alpha, \tag{49}$$

and the eigenvalues and eigenvectors of $\mathbf{B}$ are $\{s+\lambda_\alpha, \mathbf{v}_\alpha\}$. Introducing the matrix $\mathbf{V}$ whose columns are the eigenvectors,

$$\mathbf{V} = [\mathbf{v}_1 \cdots \mathbf{v}_{4N+2}], \tag{50}$$

Eq. (47) then can be written as

$$\mathbf{C}(s) = \mathbf{W}(s) \cdot \mathbf{F}(x_0), \tag{51}$$

where

$$\mathbf{W}(s) = \mathbf{V} \cdot (s\mathbf{I}+\mathbf{\Lambda})^{-1} \cdot \mathbf{V}^{-1}, \tag{52}$$

and $(\mathbf{\Lambda})_{\alpha,\beta} = \delta_{\alpha,\beta}\lambda_\alpha$. From Eqs. (40) and (51), we have

$$\tilde{\mathsf{P}}(x,s|x_0) = \mathbf{F}(x)^\dagger \cdot \mathbf{W}(s) \cdot \mathbf{F}(x_0) \tag{53}$$

or

$$\tilde{P}_{nm}(x,s|x_0) = \sum_{k,l=-N}^{N} e^{2\pi i(kx-lx_0)} [\mathbf{W}(s)]_{\alpha,\beta}. \tag{54}$$

Since $(s\mathbf{I}+\mathbf{\Lambda})^{-1}$ is diagonal, Eq. (53) can be Laplace inverted easily, and we finally have

$$\mathsf{P}(x,t|x_0,0) = \mathbf{F}(x)^\dagger \cdot \mathbf{V} \cdot e^{-\mathbf{\Lambda}t} \cdot \mathbf{V}^{-1} \cdot \mathbf{F}(x_0) \tag{55}$$

or

$$P_{nm}(x,t|x_0,0) = \sum_{k,l=-N}^{N} e^{2\pi i(kx-lx_0)} (\mathbf{V} \cdot e^{-\mathbf{\Lambda}t} \cdot \mathbf{V}^{-1})_{\alpha,\beta}. \tag{56}$$

The relaxation behavior of P is thus closely linked to the eigenvalue spectrum of the matrix $\mathbf{L}$, which is made clearer by rewriting Eq. (56) as

$$P_{nm}(x,t|x_0,0) = \sum_{\gamma} e^{-\lambda_\gamma t} \sum_{k,l} e^{2\pi i(kx-lx_0)} V_{\alpha,\gamma} V^{-1}_{\gamma,\beta}. \tag{57}$$

Equations (12) and (13), in particular, imply that $\lambda=0 \equiv \lambda_1$ is the eigenvalue whose eigenvector gives the stationary solution. Retaining only the term $\lambda_1=0$ in the first summation in Eq. (57), we write

$$\bar{P}_n(x) = \sum_k e^{2\pi ikx} V_{\alpha,1} \sum_l e^{-2\pi ilx_0} V^{-1}_{1,\beta}. \tag{58}$$

Imposing the normalization condition (28), we have

$$\sum_n V_{2N+n,1} \sum_l e^{-2\pi ilx_0} V^{-1}_{1,\beta} = 1. \tag{59}$$

Using Eq. (59) for the second summation in Eq. (58) we obtain

$$\bar{P}_n(x) = N_v \sum_k e^{2\pi ikx} V_{\alpha,1}, \tag{60}$$

where

$$N_v = \frac{1}{V_{2N+1,1} + V_{2N+2,1}}. \tag{61}$$

V. RELAXATION BEHAVIOR

A. Model potentials

Two model potentials have been used in our application: a "sawtooth" potential,

$$G_1^{(0)}(x) = \begin{cases} a(x_s - x) & (0 \leqslant x \leqslant x_s), \\ b(x - x_s) & (x_s \leqslant x \leqslant 1), \end{cases}$$

$$G_2^{(0)}(x) = g, \tag{62}$$

where $a \geqslant 0$ and $b = ax_s/(1-x_s)$ such that $G_1^{(0)}$ is periodic, and an "asymmetric cosine" potential (similar to Fig. 1),

$$G_1^{(0)}(x) = \begin{cases} \dfrac{a}{2}\left(\cos\dfrac{\pi x}{x_s} + 1\right) & (0 \leqslant x \leqslant x_s), \\ \dfrac{a}{2}\left(\cos\dfrac{\pi(1-x)}{1-x_s} + 1\right) & (x_s \leqslant x \leqslant 1), \end{cases}$$

$$G_2^{(0)}(x) = g. \tag{63}$$

In both potentials, the level $n=2$ is flat for simplicity. The sawtooth potential (62) has been used widely in other studies of ratchet models [5,6] and has the advantage of allowing analytical calculation of P for special cases (Appendix C), which we use for testing the numerical method. The dynamical variable $G_n'(x)$ to be averaged for velocity in Eq. (27), however, is discontinuous at $x=0$ and $x=x_s$ for Eq. (62). The asymmetric cosine potential (63) has a similar but smoother topology, and is more realistic. The matrix elements given by Eq. (43) for the two model potentials can be calculated analytically (Appendix B).

B. Convergence test

We first test the convergence of Fourier expansion (40) by comparing Eq. (54) with the exact expression given by Eq. (C3) for the sawtooth potential. Numerical solutions to the eigenvalue equation (48) can efficiently be obtained using the LAPACK routine "zgeev" [26] for non-Hermitian complex matrices. Since the eigenvector matrix is not unitary, the

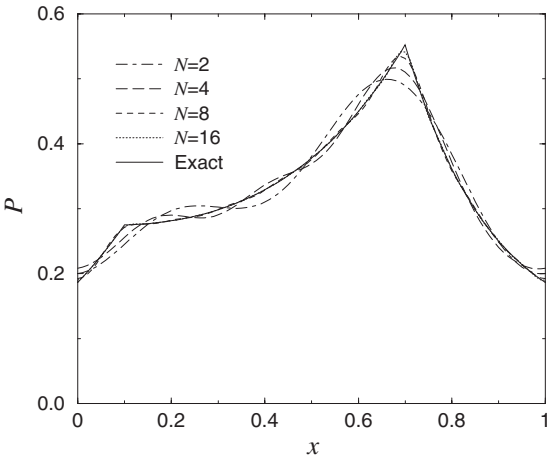

FIG. 2. Laplace transformed conditional probability density $\tilde{P}(x,s|x_0)$ as a function of x for a decoupled level of the sawtooth potential (62). Convergence of the numerical expansion (54) to the analytical exact result given by Eq. (C3) are shown with increasing N. The parameter values are $a=2$, $x_s=0.7$, $x_0=0.1$, and $s=3$.

inverse $\mathbf{V}^{-1}$ is calculated via the routines "zgetrf" and "zgetri." Figure 2 shows an example of the convergence of $\tilde{P}(x,s|x_0)$ as a function of x for a given s value.

Equation (60) provides a way of calculating the stationary distribution numerically. The convergence of this numerical result to the exact analytical expression given by Eq. (15) was tested (Fig. 3) for the asymmetric cosine potential (63) with a representative nonequilibrium condition where $z>0$ and $f_0\neq 0$. For this condition, the system is far from equilibrium due to k_2 larger than its detailed balance value, causing the population inversion of $n=1$ and $n=2$ levels. The root-mean-square errors of the results for $\tilde{P}(x,s|x_0)$ and $\bar{P}_m(x)$

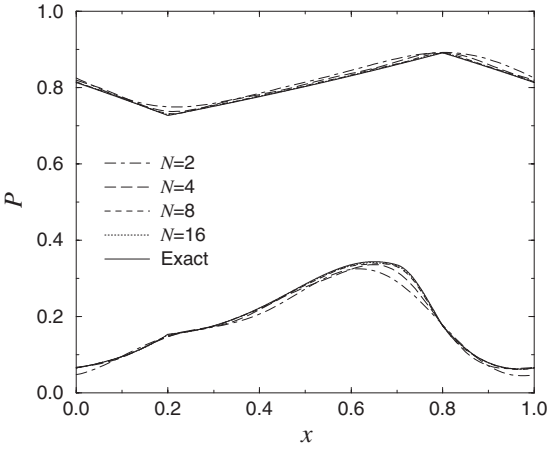

FIG. 3. Stationary probability density $\bar{P}_m(x)$ ($m=1$ and $m=2$ are the bottom and top groups, respectively) for the asymmetric cosine potential (63). The rate constants are $k_1=1.0$, $k_2^{(0)}=0.1$, with the reverse rates given by Eqs. (26). Parameters for the potential are $a=2$, $g=3$, $x_s=0.7$, $x_1=0.2$, $x_2=0.8$, and $f_0=0.5$. The parameter $z=100$ is producing a far from equilibrium condition with a population inversion. The set of numerical results with increasing N were calculated using Eq. (60). The solid lines show the exact solution given by Eq. (15).

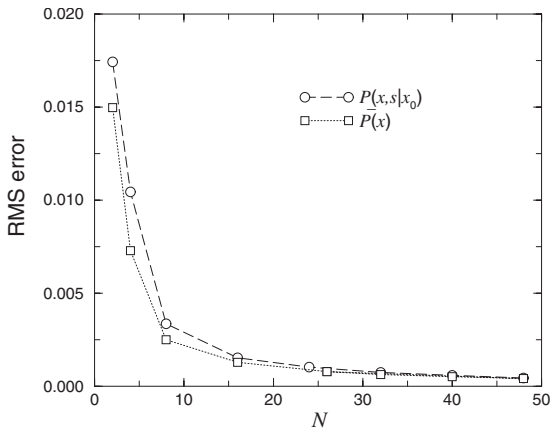

FIG. 4. Root-mean-square errors of $\tilde{P}(x,s|x_0)$ and $\bar{P}_m(x)$ of the data shown in Figs. 2 and 3 with increasing N.

shown in Fig. 4 suggest that the numerical results in general converge rapidly.

C. Relaxation of conditional probability

Figure 5 illustrates a typical relaxation behavior of $\mathsf{P}(x,t|x_0,0)$ calculated by Eq. (57) for the asymmetric cosine potential, where the density profiles evolve from the initial condition (4) to the asymptotic limit (12). The rate constants were chosen such that k_2 is larger than the value corresponding to detailed balance, resulting in a net flux $n=2\leftarrow 1$ at x_2 and the opposite flux at x_1. If the initial level is $n=1$ [Fig. 5(a)], for instance, population of the level $n=2$ does not rise appreciably until the system reaches the reaction location x_2 from x_0 via relaxations on the level $n=1$. This time scale is the characteristic relaxation time of the decoupled level $n=1$, which for the flat potential is $\tau_0=1/4\pi^2\sim O(10^{-2})$ [Eq. (C10)]. The overall relaxation of the two coupled levels therefore takes longer than the decoupled case [$\tau\sim O(10^{-1})$ in Fig. 5]. Furthermore, it is reasonable to expect that since the establishment of the stationary distribution requires interlevel transitions, the relaxation time would largely depend on the reactive flux r_0: The increase of r_0 together with velocity v_0 away from equilibrium would reduce the relaxation time.

D. Response function

Using Eq. (56), the response function given by Eq. (34) can be written as

$$R(t)=\delta(t)+(\tilde{\mathbf{G}}')^{\dagger}\cdot\mathbf{V}\cdot e^{-\mathbf{\Lambda}t}\cdot\mathbf{V}^{-1}\cdot\tilde{\mathbf{P}}', \tag{64}$$

where

$$(\tilde{\mathbf{G}}')_{\alpha}=\int_0^1 dx e^{-2\pi ikx}G_n'(x)\equiv\hat{G}_{\alpha} \tag{65}$$

and

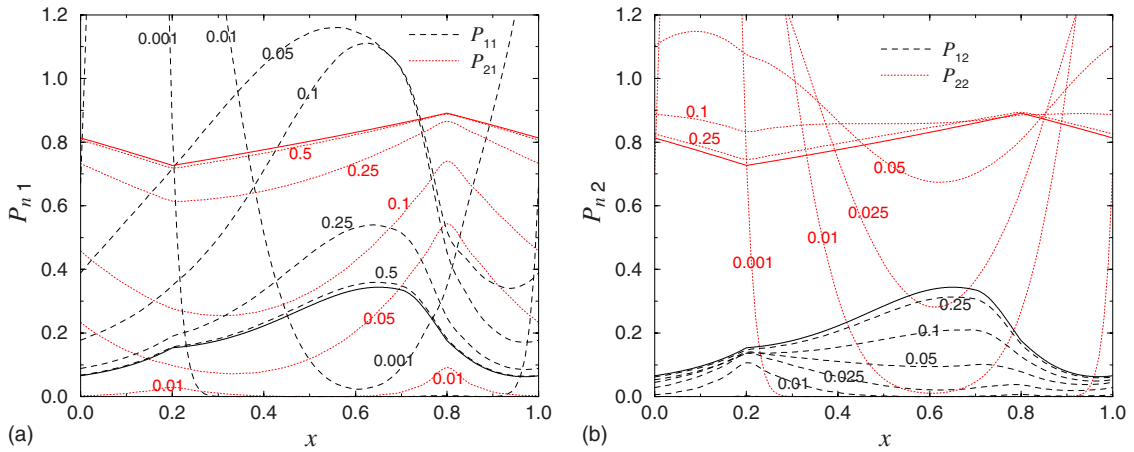

FIG. 5. (Color online) Relaxation of $P_{nm}(x,t|x_0,0)$ as a function of x and t. Initial conditions are $x_0=0.1$ and (a) $m=1$, (b) $m=2$. Parameter values for the asymmetric cosine potential are the same as in Fig. 3. Numbers on dotted and dashed lines indicate the time t. Solid lines are the stationary profiles given by Eq. (15).

$$(\tilde{\mathbf{P}}')_\alpha = \int_0^1 dx e^{-2\pi ikx}\bar{P}_n'(x) = 2\pi ik\int_0^1 dx e^{-2\pi ikx}\bar{P}_n(x) = 2\pi ikN_v V_{\alpha,1}, \quad (66)$$

where Eq. (60) was used in the second line. Equation (64) can be then written as

$$R(t) = \delta(t) + 2\pi iN_v \sum_{\alpha,\beta}\sum_{\gamma\geqslant 2} \hat{G}_\alpha^* V_{\alpha,\gamma} e^{-\lambda_\gamma t} V_{\gamma,\beta}^{-1} l V_{\beta,1}, \quad (67)$$

where we omitted the zero eigenvalue term; although $\mathbf{V}$ is not necessarily unitary, we found that the contribution from $\lambda_1=0$ always vanishes, and $R(\infty)=0$.

As a special case, the static response of velocity to force is given by

$$R_s = \frac{\partial v_0}{\partial f_0} = \int_0^\infty dt R(t), \quad (68)$$

which becomes the mobility $\mu=v_0/f_0$ when $f_0\to 0$. From Eq. (67),

$$R_s = 1 + 2\pi iN_v \sum_{\alpha,\beta}\sum_{\gamma\geqslant 2} \hat{G}_\alpha^* V_{\alpha,\gamma}\lambda_\gamma^{-1} V_{\gamma,\beta}^{-1} l V_{\beta,1}. \quad (69)$$

The exact expression for the stationary velocity, Eq. (18), also has its numerical counterpart: From Eqs. (27) and (60),

$$v_0 = -N_v \sum_\alpha \hat{G}_\alpha^* V_{\alpha,1}. \quad (70)$$

The dependence of R_s on f_0 is illustrated in Fig. 6. Equation (69) and Eqs. (18) and (68) give yet another route of checking the consistency of the numerical method with the exact solution, illustrated with one set of data in Fig. 6 where Eq. (69) with $N=32$ gives essentially exact results. Figure 7 shows the dependence of R_s on z representing the deviation from equilibrium via Eq. (25). In the absence of the dissipative media ($G_n=0$), $R_s=1$ from Eq. (69), which corresponds to the standard overdamped response of velocity to force ($\delta v=\eta^{-1}\delta f_0$ in the physical units). Dissipation generally reduces the overall velocity response from unity. The amount of this dissipative reduction is seen to decrease in Figs. 6 and 7 as one goes farther away from equilibrium with increasing z or f_0.

Time dependence of this response is given by the velocity response function, Eq. (67), whose generic shape (Fig. 8) consists of the inertial instantaneous response at $t=0$, and the dissipative contribution which is negative in sign and decays exponentially in time. An example of the velocity response arising from this response function is illustrated in Fig. 8(b) for the step function perturbation $h(t)=\Theta(t)$. For smoother forms of perturbations likely encountered in experiments, $v(t)$ would exhibit different shapes without the cusp at $t=0$.

E. Relaxation time

Figure 9 shows the relaxation behavior of $-R(t)$ for a set of parameters with equilibrium ($z=0$) and nonequilibrium

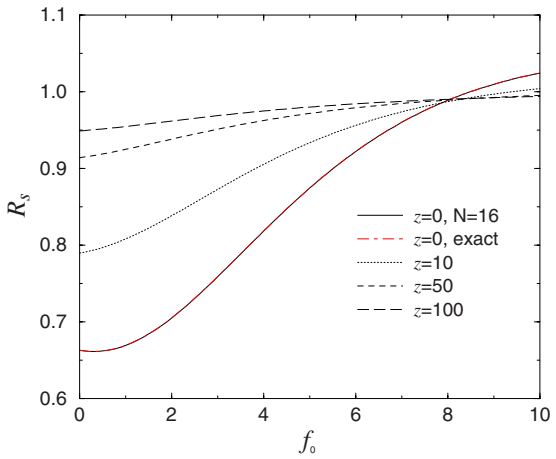

FIG. 6. (Color online) Static velocity response R_s as a function of static force f_0. The asymmetric cosine potential (63) was used with different z and f_0 values, and the rest of the parameters as in Fig. 3. $z=0$ corresponds to the equilibrium condition at $f_0=0$. The long dashed red line is from $R_s=\partial v_0/\partial f_0$ with Eq. (18), nearly indistinguishable from the numerical result via Eq. (69) with $N=16$. The rest of the data are from Eq. (69) with $N=32$.

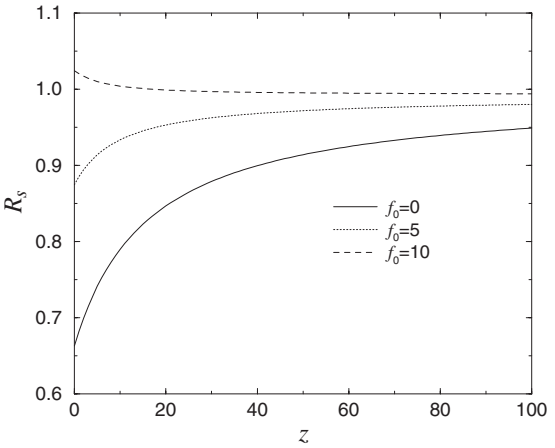

FIG. 7. Static velocity response R_s as a function of z. The parameter values are the same as for Fig. 6.

$(z>0)$ conditions. As t becomes large, the relaxation becomes dominated by contributions due to eigenvalues with lowest nonzero real part in Eq. (67). With the eigenvalues and eigenvectors ordered such that $\mathrm{Re}(\lambda_2)\leqslant\mathrm{Re}(\lambda_3)\leqslant\cdots$, Fig. 9 reveals the set of time scales

$$\tau_\alpha = \frac{1}{\mathrm{Re}(\lambda_\alpha)} \tag{71}$$

with $\alpha=2,3,\ldots$. Relaxations farther away from equilibrium become increasingly dominated by τ_2, which itself becomes smaller as z increases.

Dependence of the relaxation rates on model conditions can thus be examined via τ_2. In particular, we compare this dependence with those of stationary velocity and ATPase rate. The velocity v_0 given by Eqs. (18) or (70) and the

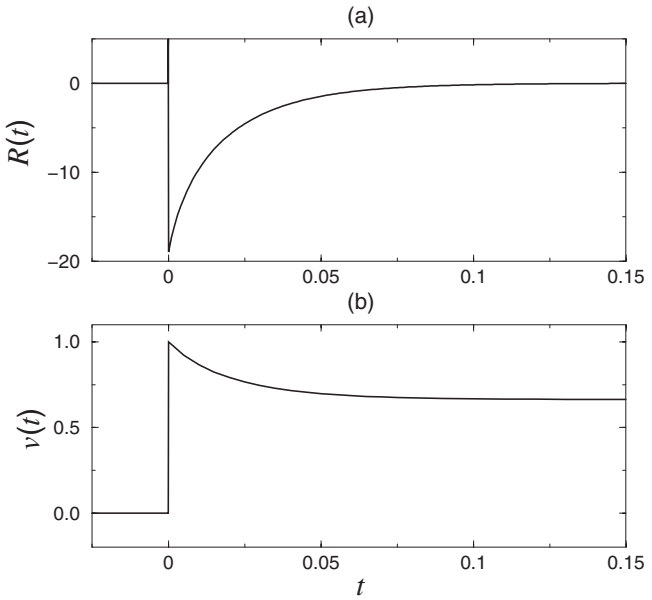

FIG. 8. Response function and an example of velocity response. (a) $R(t)$ for the parameter values same as in Fig. 6 with $f_0=0$ and $z=0$. Vertical line at $t=0$ represents the δ function. (b) $v(t)$ given by Eq. (29) with $f(t)=\Theta(t)$. $v(\infty)=R_s(f_0=0)$ in Fig. 6.

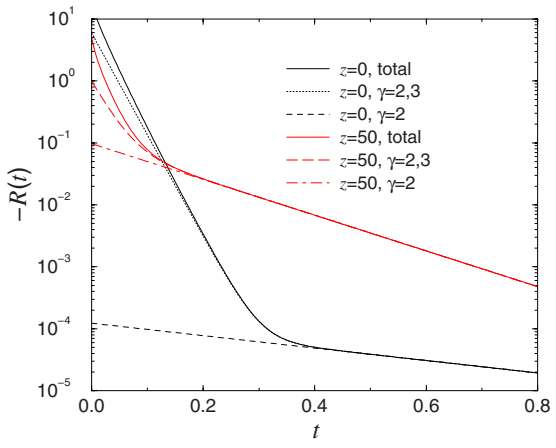

FIG. 9. (Color online) Magnitude of the nonsingular part of $R(t)$ as a function of t. The parameter values are the same as in Fig. 6 with $f_0=0$. For two values of z (equilibrium and nonequilibrium), the total response function given by Eq. (67) is shown together with the contributions of two eigenvalues with the lowest nonzero real part, λ_2 and λ_3.

reactive flux r_0 [Eq. (19)] as functions of z for fixed f_0 show the Michaelis-Menten-type behavior (Fig. 10). The relaxation time τ_2, in contrast, decreases monotonically away from equilibrium. While the absolute value of the velocity is sensitive to changes in force f_0, both r_0 and τ_2 are insensitive to the changes in force. In particular, if the time scale is plotted as a function of v_0 and r_0 instead (Fig. 11), τ_2 linearly decreases with respect to v_0 and r_0 if the departure from equilibrium is due to the chemical driving force, z. When the system is driven primarily via the mechanical driving force f_0, in contrast, τ_2 is nearly constant for a very wide range f_0, while r_0 does not change appreciably.

The fact that the dependence of characteristic relaxation time on system conditions closely follows that of the reactive flux can be understood from the requirement for interlevel crossing in the establishment of stationary distribution. A large mechanical force, resulting in high values of velocity

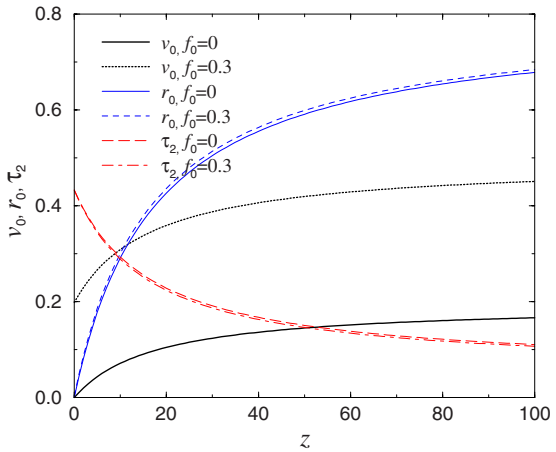

FIG. 10. (Color online) Stationary velocity v_0, reactive flux r_0 [given by Eqs. (18) or (70) and (19)], and the relaxation time τ_2 with increasing z, shown for two different values of f_0. Other parameter values are the same as in Fig. 6.

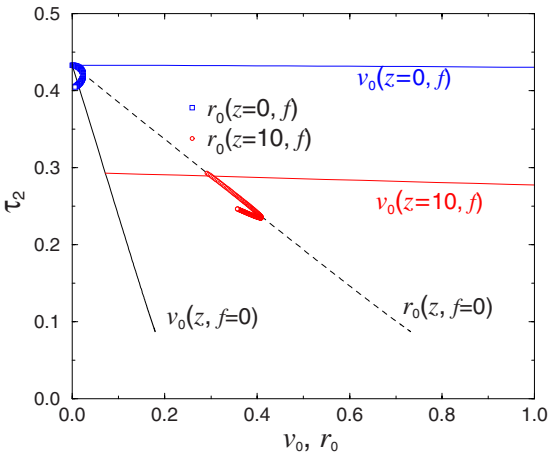

FIG. 11. (Color online) Dependence of relaxation time on velocity and reactive flux, increased in two different ways: By increasing z with $f_0=0$ (black), and by increasing f_0 for a given z ($z=0$; blue, $z=10$; red). Other parameter values are the same as in Fig. 6.

without facilitating interlevel crossing, leaves the relaxation behavior largely unaffected. This behavior quantifies the trend observed earlier in the relaxation of $\mathsf{P}(x,t|x_0,0)$ in Fig. 5, where the overall relaxation must wait until the initial distribution spreads to the reaction locations and crosses over to the other level via reactions.

VI. DISCUSSION

Brownian ratchet models directly tackle the interplay of mechanical and chemical degrees of freedom, and our general expressions of stationary velocity and ATPase rate, Eqs. (18) and (19), summarize the effects of the two different sources of nonequilibrium behavior. Our choice of model potentials [Eqs. (62) and (63)], appropriate for examining thermal ratchet effects, represents relatively loose coupling between the chemical and mechanical degrees of freedom. A velocity increase upon force can therefore be achieved without the corresponding increase in the reactive flux; the motor complex can "slide" along within each level without appreciable reactions. When the motion is being driven mainly via chemistry (high $\Delta\mu$), on the other hand, both the velocity and ATPase rate are large in magnitude. A different limit is where the chemical and mechanical parts are tightly coupled as assumed within discrete state kinetic models of molecular motors [27]. In this limit, there is no distinction between the reactive flux and velocity.

The main results of our study suggest that a Brownian ratchet responds to external perturbations with a time scale that decreases linearly with v_0 and r_0 when driven by chemical nonequilibrium conditions. When the motion is primarily due to mechanical force (v_0 large but r_0 small) the relaxation time remains largely unchanged. We expect this prediction to be testable in single molecule experiments using mechanical or spectroscopic means.

The exact solution obtained for stationary properties in Sec. III greatly aides the understanding of the model predictions. Determining the solution nevertheless becomes rapidly unmanageable with more than two levels or two reaction sites. The numerical method described in Sec. IV is easily generalized to such cases, and provides an efficient route to determine both the static and dynamical properties of related models.

ACKNOWLEDGMENT

The author thanks Joe Cline for helpful comments.

APPENDIX A: STATIONARY SOLUTION

The boundary conditions for $\bar{P}_n(x)$ are the periodicity at $x=0,1$, the continuity at $x=x_n$, and the balance of fluxes at these locations obtained by integrating Eq. (13) over an infinitesimal region near the singular points:

$$\bar{P}_n^{(1)}(0) = \bar{P}_n^{(3)}(1), \tag{A1a}$$

$$J_n^{(3)} - J_n^{(1)} = 0, \tag{A1b}$$

$$\bar{P}_n^{(1)}(x_1) = \bar{P}_n^{(2)}(x_1), \tag{A1c}$$

$$J_1^{(2)} - J_1^{(1)} = k_1\bar{P}_2^{(2)}(x_1) - k_{-1}\bar{P}_1^{(2)}(x_1), \tag{A1d}$$

$$J_2^{(2)} - J_2^{(1)} = k_{-1}\bar{P}_1^{(2)}(x_1) - k_1\bar{P}_2^{(2)}(x_1), \tag{A1e}$$

$$\bar{P}_n^{(2)}(x_2) = \bar{P}_n^{(3)}(x_2), \tag{A1f}$$

$$J_1^{(3)} - J_1^{(2)} = k_{-2}\bar{P}_2^{(3)}(x_2) - k_2\bar{P}_1^{(3)}(x_2), \tag{A1g}$$

$$J_2^{(3)} - J_2^{(2)} = k_2\bar{P}_1^{(3)}(x_2) - k_{-2}\bar{P}_2^{(3)}(x_2), \tag{A1h}$$

where $n=1,2$. From Eq. (14), we can write

$$\bar{P}_n^{(1)}(x) = e^{-G_n(x)}\left(A_n^{(1)} - J_n^{(1)}\int_0^x dx'\, e^{G_n(x')}\right),$$

$$\bar{P}_n^{(2)}(x) = e^{-G_n(x)}\left(A_n^{(2)} - J_n^{(2)}\int_{x_1}^x dx'\, e^{G_n(x')}\right),$$

$$\bar{P}_n^{(3)}(x) = e^{-G_n(x)}\left(A_n^{(3)} - J_n^{(3)}\int_{x_2}^x dx'\, e^{G_n(x')}\right). \tag{A2}$$

Using Eq. (A2) and $G_n(1)=G_n(0)-f_0$, the boundary conditions (A1) become

$$e^{-f_0}A_1^{(1)} = A_1^{(3)} - u_1J_1^{(3)}, \tag{A3a}$$

$$e^{-f_0}A_2^{(1)} = A_2^{(3)} - u_2J_2^{(3)}, \tag{A3b}$$

$$J_1^{(1)} = J_1^{(3)}, \tag{A3c}$$

$$J_2^{(1)} = J_2^{(3)}, \tag{A3d}$$

$$A_1^{(1)} - w_1 J_1^{(1)} = A_1^{(2)}, \tag{A3e}$$

$$A_2^{(1)} - w_2 J_2^{(1)} = A_2^{(2)}, \tag{A3f}$$

$$J_1^{(2)} - J_1^{(1)} = d_2 k_1 A_2^{(2)} - d_1 k_{-1} A_1^{(2)}, \tag{A3g}$$

$$J_2^{(2)} - J_2^{(1)} = d_1 k_{-1} A_1^{(2)} - d_2 k_1 A_2^{(2)}, \tag{A3h}$$

$$A_1^{(2)} - h_1 J_1^{(2)} = A_1^{(3)}, \tag{A3i}$$

$$A_2^{(2)} - h_2 J_2^{(2)} = A_2^{(3)}, \tag{A3j}$$

$$J_1^{(3)} - J_1^{(2)} = c_2 k_{-2} A_2^{(3)} - c_1 k_2 A_1^{(3)}, \tag{A3k}$$

$$J_2^{(3)} - J_2^{(2)} = c_1 k_2 A_1^{(3)} - c_2 k_{-2} A_2^{(3)}. \tag{A3l}$$

Only 11 of 12 relations in Eqs. (A3) are independent, since Eqs. (A3c)+(A3d)+(A3g)+(A3h)+(A3k)+(A3l)=0. These 11 relations and the normalization condition determine the 12 coefficients, $\{A_n^{(j)}, J_n^{(j)}\}$ for $n=1,2$ and $j=1,2,3$. Alternatively, we can set one of the coefficients arbitrarily in terms of the normalization constant A and determine the rest using the 11 boundary conditions: We choose $A_1^{(2)}=A$.

We first eliminate $A_n^{(1)}, J_n^{(1)}$ in Eqs. (A3e)–(A3h) using Eqs. (A3a)–(A3d),

$$e^{f_0} A_1^{(3)} - (e^{f_0} u_1 + w_1) J_1^{(3)} = A, \tag{A4a}$$

$$e^{f_0} A_2^{(3)} - (e^{f_0} u_2 + w_2) J_2^{(3)} = A_2^{(2)}, \tag{A4b}$$

$$J_1^{(2)} - J_1^{(3)} = d_2 k_1 A_2^{(2)} - d_1 k_{-1} A, \tag{A4c}$$

$$J_2^{(2)} - J_2^{(3)} = d_1 k_{-1} A_1^{(2)} - d_2 k_1 A_2^{(2)}. \tag{A4d}$$

From Eqs. (A4a), (A4b), (A3i), and (A3j) we have

$$J_1^{(3)} = \frac{1}{w_1 + u_1 e^{f_0}} (e^{f_0} A_1^{(3)} - A), \tag{A5a}$$

$$J_2^{(3)} = -\frac{1}{w_2 + u_2 e^{f_0}} (A_2^{(2)} - e^{f_0} A_2^{(3)}), \tag{A5b}$$

$$J_1^{(2)} = \frac{1}{h_1} (A - A_1^{(3)}), \tag{A5c}$$

$$J_2^{(2)} = \frac{1}{h_2} (A_2^{(2)} - A_2^{(3)}). \tag{A5d}$$

Substituting Eqs. (A5a)–(A5d) into Eqs. (A3k), (A3l), and (A4c), we obtain

$$c_2 k_{-2} A_2^{(3)} - (c_1 k_2 + m_1) A_1^{(3)} + m_1' A = 0, \tag{A6a}$$

$$(m_2 + c_2 k_{-2}) A_2^{(3)} - m_2' A_2^{(2)} - c_1 k_2 A_1^{(3)} = 0, \tag{A6b}$$

$$(m_1' + d_1 k_{-1}) A - m_1 A_1^{(3)} - d_2 k_1 A_2^{(2)} = 0. \tag{A6c}$$

Equation (A6c) gives

$$A_1^{(3)} = [(m_1' + d_1 k_{-1}) A - d_2 k_1 A_2^{(2)}]/m_1, \tag{A7}$$

which can be substituted into Eq. (A6b) to give

$$A_2^{(3)} = \frac{(c_1 d_1 k_2 k_{-1} + m_1' c_1 k_2) A + (m_1 m_2' - c_1 k_2 d_2 k_1) A_2^{(2)}}{m_1 (m_2 + c_2 k_{-2})}. \tag{A8}$$

We then substitute Eqs. (A7) and (A8) into Eq. (A6a) and solve for $A_2^{(2)}$, which yields after some algebra,

$$A_2^{(2)} = AL/Q, \tag{A9}$$

where L and Q are given by Eqs. (17b) and (17c). Equation (A9) substituted into Eq. (A8) gives

$$A_2^{(3)} = AM/Q, \tag{A10}$$

where M is given by Eq. (17a). Using Eq. (A9) in Eq. (A7) and simplifying, one obtains

$$A_1^{(3)} = A \frac{m_1'}{m_1} \left(1 - \frac{m_2}{Q} \Gamma_1\right), \tag{A11}$$

where Γ_1 is given by Eq. (16a). Equations (A5c) and (A11) now yield

$$J_1^{(2)}/A = -\frac{1}{h_1} \left(\frac{m_1'}{m_1} - 1\right) + \frac{m_1' m_2 \Gamma_1}{m_1 h_1 Q} = \frac{1 - e^{-f_0}}{g_1 + h_1} + \frac{m_1' m_2 \Gamma_1}{m_1 h_1 Q}, \tag{A12}$$

and Eqs. (A5d), (A9), and (A10) give

$$J_2^{(2)} = \frac{A}{h_2 Q} \left(\frac{1 - e^{-f_0}}{g_2} F - m_1' \Gamma_2\right), \tag{A13}$$

where F and Γ_2 are given by Eqs. (17d) and (16b), respectively. From Eqs. (A5a) and (A11) we have

$$J_1^{(3)}/A = \frac{1 - e^{-f_0}}{g_1 + h_1} - \frac{m_1' m_2 \Gamma_1}{m_1 g_1 Q}, \tag{A14}$$

while Eqs. (A5b), (A9), and (A10) yield

$$J_2^{(3)} = \frac{A}{g_2 Q} \left(\frac{1 - e^{-f_0}}{h_2} F + m_1' \Gamma_3\right), \tag{A15}$$

where Γ_3 is given by Eq. (16c). Equation (A3e) gives

$$A_1^{(1)}/A = 1 + \frac{(1 - e^{-f_0}) w_1}{g_1 + h_1} - \frac{w_1 m_1' m_2}{m_1 g_1 Q} \Gamma_1, \tag{A16}$$

and finally Eq. (A3b),

$$A_2^{(1)} = \frac{A}{Q} \left(e^{f_0} M + \frac{(1 - e^{f_0}) u_2 F}{g_2 h_2} - \frac{e^{f_0} u_2 m_1'}{g_2} \Gamma_3\right). \tag{A17}$$

Equations (A16), (A3c), (A12), (A14), (A11), (A17), (A3d), (A9), (A13), (A10), and (A15) complete the solution written as Eq. (15).

The stationary velocity v_0 can be evaluated as $v_0 = J_1^{(j)} + J_2^{(j)}$ for any j, since the total flux is independent of x. Choosing $j=2$ directly yields Eq. (18). The reactive flux r_0, defined as the flux $n=2 \leftarrow 1$ at x_2, can be obtained as $r_0 = J_1^{(2)} - J_1^{(3)}$, which gives Eq. (19).

APPENDIX B: MATRIX ELEMENTS

From Eq. (8), the matrix elements (43) for the sawtooth potential (62) can be calculated as

$$(\Omega_{kl})_{11} = (a+b)[1+(1-\delta_{kl})l/(k-l)](1-e^{2\pi i(l-k)x_s}) + \delta_{kl}(4\pi^2 l^2 + 2\pi i l f_0),$$

$$(\Omega_{kl})_{22} = \delta_{kl}(4\pi^2 l^2 + 2\pi i l f_0), \tag{B1}$$

and $(\Omega_{kl})_{12}=(\Omega_{kl})_{21}=0$. For the asymmetric cosine potential (63),

$$(\Omega_{kl})_{11} = \frac{\pi i a}{4}\left[(2l+x_s^{-1})z_{l-k}(x_s) + (2l-x_s^{-1})z^*_{k-l}(x_s) - \left(2l+\frac{1}{1-x_s}\right)z^*_{l-k}(1-x_s) - \left(2l-\frac{1}{1-x_s}\right)z_{k-l}(1-x_s)\right] + \delta_{kl}(4\pi^2 l^2 + 2\pi i l f_0),$$

$$(\Omega_{kl})_{22} = \delta_{kl}(4\pi^2 l^2 + 2\pi i l f_0), \tag{B2}$$

and $(\Omega_{kl})_{12}=(\Omega_{kl})_{21}=0$, where

$$z_k(x) = \begin{cases} \dfrac{1+e^{2\pi i k x}}{1+2kx} & \text{if } kx \neq -1/2, \\ -\pi i & \text{if } kx = -1/2. \end{cases} \tag{B3}$$

Elements of the vector $\tilde{\mathbf{G}}'$ in Eq. (65) for this potential can also be written in terms of $z_k(x)$,

$$(\tilde{\mathbf{G}}')_{2(k+N)+1} = \frac{ak}{2}[x_s z^*_k(x_s) - x_s z_{-k}(x_s) + (1-x_s)z^*_{-k}(1-x_s) - (1-x_s)z_k(1-x_s)] - f_0\delta_{k0},$$

$$(\tilde{\mathbf{G}}')_{2(k+N)+2} = -f_0\delta_{k0}. \tag{B4}$$

APPENDIX C: SAWTOOTH POTENTIAL

The Laplace transform $\tilde{P}\equiv\tilde{P}_{11}(x,s|x_0)$ can be obtained analytically for a decoupled level $n=1$ of the sawtooth potential (62). Equation (38) in this case becomes

$$\tilde{P}'' + G_1'\tilde{P}' + (G_1'' - s)\tilde{P} + \delta(x-x_0) = 0, \tag{C1}$$

where $\tilde{P}'=d\tilde{P}/dx$ and $\tilde{P}''=d^2\tilde{P}/dx^2$. General solutions each containing two multiplicative coefficients can be written for three nonsingular regions $(x\neq 0,1,x_s,x_0)$. The boundary conditions determining the coefficients are analogous to Eq. (A1),

$$\tilde{P}(0) = \tilde{P}(1),$$

$$\tilde{P}(x_s^-) = \tilde{P}(x_s^+),$$

$$\tilde{P}'(0) - \tilde{P}'(1) = [G_1'(1) - G_1'(0)]\tilde{P}(0),$$

$$\tilde{P}'(x_s^+) - \tilde{P}'(x_s^-) = [G_1'(x_s^-) - G_1'(x_s^+)]\tilde{P}(x_s),$$

$$\tilde{P}'(x_0^+) - \tilde{P}'(x_0^-) + 1 = 0,$$

$$\tilde{P}(x_0^+) = \tilde{P}(x_0^-). \tag{C2}$$

1. General case

We only quote the results for the Laplace transform $\tilde{P}(x,s|x_0)$ obtained by imposing the boundary conditions (C2), divided into two cases: For $0\leqslant x_0\leqslant x_s$,

$$\tilde{P} = \begin{cases} \dfrac{e^{a(x-x_0)/2}}{2s_a\gamma}(A_1 e^{s_a x} + B_1 e^{-s_a x}) & (0\leqslant x\leqslant x_0), \\ \dfrac{e^{a(x-x_0)/2}}{2s_a\gamma}(A_1' e^{s_a x} + B_1' e^{-s_a x}) & (x_0\leqslant x\leqslant x_s), \\ \dfrac{e^{[b(1-x)-ax_0]/2}}{\gamma}(C_1 e^{s_b(x-1)} + D_1 e^{s_b(1-x)}) & (x_s\leqslant x\leqslant 1), \end{cases} \tag{C3}$$

where

$$A_1 = 2s_a s_b\{e^{-x_0 s_a} - e^{(x_s-x_0)s_a}\,\mathrm{ch}[(1-x_s)s_b]\} - (a+b)\left(s_a+\frac{a}{2}\right)e^{-(x_s-x_0)s_a}\,\mathrm{sh}[(1-x_s)s_b] - \left(2s-\frac{ab}{2}\right)e^{(x_s-x_0)s_a}\,\mathrm{sh}[(1-x_s)s_b],$$

$$B_1 = -2s_a s_b\{e^{x_0 s_a} - e^{-(x_s-x_0)s_a}\,\mathrm{ch}[(1-x_s)s_b]\} + (a+b)\left(s_a-\frac{a}{2}\right)e^{(x_s-x_0)s_a}\,\mathrm{sh}[(1-x_s)s_b] - \left(2s-\frac{ab}{2}\right)e^{-(x_s-x_0)s_a}\,\mathrm{sh}[(1-x_s)s_b],$$

$$A_1' = -2s_a s_b\{e^{-x_0 s_a} - \mathrm{ch}[(1-x_s)s_b]e^{-(x_s+x_0)s_a}\} - (a+b)\left(s_a+\frac{a}{2}\right)e^{-(x_s-x_0)s_a}\,\mathrm{sh}[(1-x_s)s_b] - \left(2s-\frac{ab}{2}\right)e^{-(x_s+x_0)s_a}\,\mathrm{sh}[(1-x_s)s_b],$$

$$B_1' = 2s_a s_b\{e^{x_0 s_a} - \mathrm{ch}[(1-x_s)s_b]e^{(x_s+x_0)s_a}\} + (a+b)\left(s_a-\frac{a}{2}\right)e^{(x_s-x_0)s_a}\,\mathrm{sh}[(1-x_s)s_b] - \left(2s-\frac{ab}{2}\right)e^{(x_s+x_0)s_a}\,\mathrm{sh}[(1-x_s)s_b],$$

$$C_1 = -\left(s_b-\frac{a+b}{2}\right)\{\mathrm{sh}(x_0 s_a) + e^{(1-x_s)s_b}\,\mathrm{sh}[(x_s-x_0)s_a]\} + s_a\,\mathrm{ch}(x_0 s_a) - e^{(1-x_s)s_b}s_a\,\mathrm{ch}[(x_s-x_0)s_a],$$

$$D_1 = -\left(s_b + \frac{a+b}{2}\right)\{\mathrm{sh}(x_0 s_a) + e^{-s_b(1-x_s)}\,\mathrm{sh}[(x_s - x_0)s_a]\}$$
$$- s_a\,\mathrm{ch}(x_0 s_a) + e^{-(1-x_s)s_b} s_a\,\mathrm{ch}[(x_s - x_0)s_a], \tag{C4}$$

ch $z=\cosh z$, sh $z=\sinh z$, $s_a=(s+a^2/4)^{1/2}$, $s_b=(s+b^2/4)^{1/2}$, and

$$\gamma = 4 s_a s_b\{1 - \mathrm{ch}(x_s s_a)\mathrm{ch}[(1-x_s)s_b]\}$$
$$- (4s - ab)\mathrm{sh}(x_s s_a)\mathrm{sh}[(1-x_s)s_b]. \tag{C5}$$

For $x_s \leqslant x_0 \leqslant 1$,

$$\tilde{P} = \begin{cases} \dfrac{e^{(bx_0+ax-b)/2}}{\gamma}(A_2 e^{s_a x} + B_2 e^{-s_a x}) & (0 \leqslant x \leqslant x_s), \\ \dfrac{e^{b(x_0-x)/2}}{2s_b\gamma}(C_2 e^{s_b x} + D_2 e^{-s_b x}) & (x_s \leqslant x \leqslant x_0), \\ \dfrac{e^{b(x_0-x)/2}}{2s_b\gamma}(C_2' e^{s_b(x-1)} + D_2' e^{s_b(1-x)}) & (x_0 \leqslant x \leqslant 1), \end{cases} \tag{C6}$$

where

$$A_2 = -\left(s_a + \frac{a+b}{2}\right)\{\mathrm{sh}[(x_0 - x_s)s_b]e^{-x_s s_a} + \mathrm{sh}[(1-x_0)s_b]\}$$
$$+ s_b\{\mathrm{ch}[(x_0 - x_s)s_b]e^{-x_s s_a} - \mathrm{ch}[(1-x_0)s_b]\},$$

$$B_2 = -\left(s_a - \frac{a+b}{2}\right)\{\mathrm{sh}[(x_0 - x_s)s_b]e^{x_s s_a} + \mathrm{sh}[(1-x_0)s_b]\}$$
$$- s_b\{\mathrm{ch}[(x_0 - x_s)s_b]e^{x_s s_a} - \mathrm{ch}[(1-x_0)s_b]\},$$

$$C_2 = 2 s_a s_b[e^{-x_0 s_b} - e^{(1-x_s-x_0)s_b}\,\mathrm{ch}(x_s s_a)]$$
$$+ (a+b)(s_b - b/2)e^{(x_0-x_s-1)s_b}\,\mathrm{sh}(x_s s_a)$$
$$- e^{-(x_0+x_s-1)s_b}(2s - ab/2)\mathrm{sh}(x_s s_a),$$

$$D_2 = -2 s_a s_b[e^{x_0 s_b} - e^{-(1-x_s-x_0)s_b}\,\mathrm{ch}(x_s s_a)]$$
$$- (a+b)(s_b + b/2)e^{-(x_0-x_s-1)s_b}\,\mathrm{sh}(x_s s_a)$$
$$- e^{(x_0+x_s-1)s_b}(2s - ab/2)\mathrm{sh}(x_s s_a),$$

$$C_2' = -2 s_a s_b[e^{(1-x_0)s_b} - e^{-(x_0-x_s)s_b}\,\mathrm{ch}(x_s s_a)]$$
$$+ (a+b)(s_b - b/2)$$
$$\times e^{(x_0-x_s)s_b}\,\mathrm{sh}(x_s s_a) - (2s - ab/2)e^{-(x_0-x_s)s_b}\,\mathrm{sh}(x_s s_a),$$

$$D_2' = 2 s_a s_b[e^{-(1-x_0)s_b} - e^{(x_0-x_s)s_b}\,\mathrm{ch}(x_s s_a)] - (a+b)(s_b$$
$$+ b/2)e^{-(x_0-x_s)s_b}\,\mathrm{sh}(x_s s_a) - (2s - ab/2)e^{(x_0-x_s)s_b}\,\mathrm{sh}(x_s s_a). \tag{C7}$$

2. Flat potential

If $a=0$, $\tilde{P}(x,s|x_0)$ simplifies considerably,

$$\tilde{P} = \frac{(1 - e^{\sqrt{s}})e^{-\sqrt{s}|x-x_0|} + (e^{-\sqrt{s}} - 1)e^{\sqrt{s}|x-x_0|}}{4\sqrt{s}(1 - \cosh\sqrt{s})}. \tag{C8}$$

This special case allows for analytical Laplace inversion via

$$P(x,t|x_0,0) = \frac{1}{2\pi i}\int_{c-i\infty}^{c+i\infty} ds e^{st}\tilde{P}(x,s|x_0), \tag{C9}$$

where c is real and larger than real parts of any singular points in the complex plane. The branch cut can be chosen as the negative real axis, and the singularities all lie on this axis at $s=-(2n\pi)^2$, $n=0,1,2,\ldots$. The line integrals along the branch cut cancel out, and one can obtain

$$P(x,t|x_0,0) = 1 + 2\sum_{n=1}^{\infty} e^{-(2\pi n)^2 t}\cos[2n\pi(x - x_0)]. \tag{C10}$$

It is readily seen that this solution satisfies $P(x,0|x_0,0) = \delta(x - x_0)$ and $P(x,\infty|x_0,0)=1$.

This result for the flat potential can also be verified from the eigenvector matrix representation, Eq. (56). When $a=0$, from Eqs. (8) and (9) we have $\hat{\mathsf{L}}_0(x)=\hat{\sigma}_x^2\mathsf{I}$, and Eq. (46a) becomes $(\mathbf{L})_{\alpha,\beta}=-4\pi^2k^2\delta_{kl}\delta_{nm}$, with Eqs. (46e) and (46f). The eigenvalues and eigenvectors are therefore $(\mathbf{\Lambda})_\alpha = 4\pi^2k^2$ and $\mathbf{V}=\mathbf{I}$. Equation (57) then yields Eq. (C10) with $n=m=1$.

[1] R. D. Vale and R. A. Milligan, Science **288**, 88 (2000).
[2] A. D. Mehta, M. Rief, J. A. Spudich, D. A. Smith, and R. M. Simmons, Science **283**, 1689 (1999).
[3] M. D. Wang, M. J. Schnitzer, H. Yin, R. Landick, J. Gelles, and S. M. Block, Science **282**, 902 (1998).
[4] S. Myong, B. C. Stevens, and T. Ha, Structure (London) **14**, 633 (2006).
[5] F. Jülicher, A. Ajdari, and J. Prost, Rev. Mod. Phys. **69**, 1269 (1997).
[6] P. Reimann, Phys. Rep. **361**, 57 (2002).
[7] P. Reimann, C. Van den Broeck, H. Linke, P. Hänggi, J. M. Rubi, and A. Pérez-Madrid, Phys. Rev. Lett. **87**, 010602 (2001).
[8] R. D. Astumian, Science **276**, 917 (1997).
[9] R. D. Astumian and M. Bier, Phys. Rev. Lett. **72**, 1766 (1994).
[10] P. Reimann, R. Bartussek, R. Häußler, and P. Hänggi, Phys. Lett. A **215**, 26 (1996).
[11] J. Prost, J. F. Chauwin, L. Peliti, and A. Ajdari, Phys. Rev. Lett. **72**, 2652 (1994).
[12] A. Parmeggiani, F. Jülicher, A. Ajdari, and J. Prost, Phys. Rev. E **60**, 2127 (1999).
[13] H. Qian, J. Phys. Chem. B **110**, 15063 (2006).
[14] H. Qian, J. Phys. Chem. B **106**, 2065 (2002).
[15] H. Qian, Phys. Rev. E **69**, 012901 (2004).
[16] M. van den Broek and C. Van den Broeck, Phys. Rev. E **78**, 011102 (2008).
[17] S. Sporer, C. Goll, and K. Mecke, Phys. Rev. E **78**, 011917 (2008).

[18] E. M. Craig, M. J. Zuckermann, and H. Linke, Phys. Rev. E **73**, 051106 (2006).
[19] L. Machura, M. Kostur, P. Talkner, J. Luczka, F. Marchesoni, and P. Hänggi, Phys. Rev. E **70**, 061105 (2004).
[20] F. J. Cao, L. Dinis, and J. M. R. Parrondo, Phys. Rev. Lett. **93**, 040603 (2004).
[21] H.-J. Woo and C. L. Moss, Phys. Rev. E **72**, 051924 (2005).
[22] H.-J. Woo, Phys. Rev. E **74**, 011907 (2006).
[23] H. Risken, *The Fokker-Planck Equation: Methods of Solution and Applications* (Springer, Berlin, 1996).
[24] N. G. van Kampen, *Stochastic Processes in Physics and Chemistry* (North-Holland, Amsterdam, 1983).
[25] G. Lattanzi and A. Maritan, Phys. Rev. Lett. **86**, 1134 (2001).
[26] E. Anderson *et al.*, *LAPACK Users' Guide*, 3rd ed. (Society for Industrial and Applied Mathematics, Philadelphia, PA, 1999).
[27] M. E. Fisher and A. B. Kolomeisky, Proc. Natl. Acad. Sci. U.S.A. **96**, 6597 (1999).